IEEE Photonics Journal
An IEEE Photonics Society Publication

Open Access

Enhancement of Optical Nonlinearity in the Triangular Gold Nanoplates on Indium Tin Oxide

Volume 13, Number 3, June 2021

Jing Huang
Jie Li
Dongyang Liu
Lili Miao
Chujun Zhao

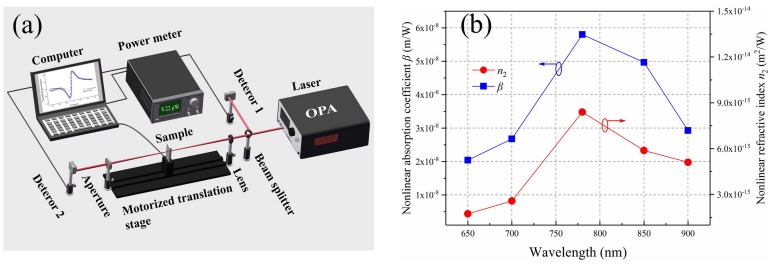

DOI: 10.1109/JPHOT.2021.3085871

IEEE photonics SOCIETY

IEEE

Enhancement of Optical Nonlinearity in the Triangular Gold Nanoplates on Indium Tin Oxide

Jing Huang, Jie Li, Dongyang Liu, Lili Miao, and Chujun Zhao

Key Laboratory for Micro/Nano Optoelectronic Devices of Ministry of Education & Hunan Provincial Key Laboratory of Low-Dimensional Structural Physics and Devices, School of Physics and Electronics, Hunan University, Changsha, Hunan 410082, China

DOI:10.1109/JPHOT.2021.3085871
This work is licensed under a Creative Commons Attribution 4.0 License. For more information, see https://creativecommons.org/licenses/by/4.0/

Manuscript received May 17, 2021; accepted May 28, 2021. Date of publication June 1, 2021; date of current version June 17, 2021. This work was supported in part by the National Natural Science Foundation of China (NSFC) under Grants 61775056, 61805076 and 61975055. Corresponding authors: Lili Miao; Chujun Zhao (lilimiao@hnu.edu.cn; cjzhao@hnu.edu.cn).

Abstract: The nonlinear optical materials with small footprint, low operating energy, ultrafast and large nonlinear optical response are highly required for the signal processing. Here, we investigated the broadband optical nonlinear response of the triangular gold nanoplates on indium tin oxide (ITO) coated glass, and obtained a large optical nonlinear enhancement at its localized surface plasmon resonance (LSPR) region at the wavelength of 780 nm, far from the ENZ (epsilon-near-zero) region of ITO. The measured nonlinear refractive index and nonlinear absorption coefficient can reach up to 8.39×10^{-15} m^2/W and 5.81×10^{-8} m/W, respectively. The experimental results highlight the noble metals' potential for nonlinear optics and nanophotonics.

Index Terms: Light interaction, nonlinear effects, Kerr effect, optical properties of photonic materials, ultrafast nonlinear process, plasmonics.

1. Introduction

Optical materials with large nonlinear optical response are highly required for the signal processing. The nonlinear optical responses of conventional materials are typically inherently weak [1], [2], which put forward changes for optical signal processing in photonics (i.e., photon generation, manipulation, transmission, detection, and imaging [1]–[5]). In addition, the size and operating energy of a nonlinear optical device are fundamentally constrained by the weak of the nonlinear optical response of common materials [6]. Over the years, several approaches have been explored to enhance the intrinsic nonlinear optical response of materials, including local field enhancement using metamaterials [7]–[10], composite structures [11]–[13], and plasmonic structures [14], [15]. Metamaterials have been predicted to enable a plethora of novel light-matter interactions [16], exhibiting an interplay of electric and magnetic-type nonlinearities [17], [18]. In another case, plasmonic nanostructures provide inside and interior local field enhancement and, as a result, nonlinear effects can be obvious, including the generation of new frequencies and ultrafast, transient variations of the fundamental wave's intensity [19]–[23]. Metallic nanoparticles deposited on transparent substrates also exhibit structure and geometry-dependent optical properties due to the occurrence of local surface plasmon resonance (LSPR) effects. For example, the transparent conductive oxide film or optical glass containing the gold nanoparticles show interesting optical properties [24], [25].

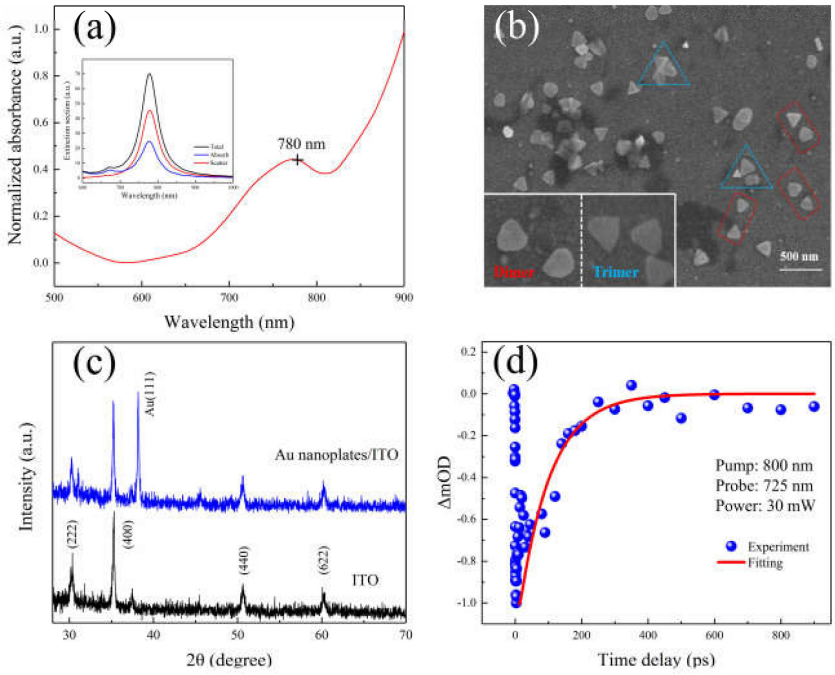

Fig. 1. (a) The measured absorption spectrum of the gold nanoplates, and the inset is the calculated extinction properties of a single gold triangular nanoplate. (b) The SEM image of gold triangular nanoplates on ITO glass. (c) The XRD pattern of ITO and gold nanoplates on ITO glass, respectively. (d) Ultrafast carrier dynamics characteristic of the triangular gold.

The excellent nonlinear optical properties of the local surface plasmon nanostructures provide a good platform for the study and applications of the nonlinear optics, such as plasmon waveguide, sensor, and nanoprobes [26]–[29].

Gold nanostructures have been extensively studied because their LSPR frequency is located in the visible spectral range. Additionally, its molecular adhesion to the surface is chemically stable [30]–[34]. Similarly, the optical materials with high transmittance also receive great attention, such as the indium tin oxide (ITO). Bernd Metzger et al. investigated the enhanced third harmonic generation by positioning ITO nanocrystals into the hot-spot of plasmonic gap-antennas [35]. Zahirul Alam et al. demonstrated a 50 nm thick optical metasurface made of optical dipole antennas and an epsilon-near-zero material ITO [36]. Ferbonink et al. studied the ultrafast dynamics response of gold triangular pyramid arrays deposited over glass [37]. Considering the high optical transmittance, good adhesion to the substrate [38]–[41], and tunable permittivity by doping or applying bias, the ITO has exhibited versatile optoelectronic performance.

Here, we have experimentally investigated the broadband third-order optical nonlinear response of the triangular gold nanoplates onto ITO glass, and the results show a large optical nonlinear enhancement at nanoplates' LSPR region. In addition, the finite-difference-time-domain method has been used to clarify the optical nonlinearity enhancement mechanism. Our results show the potential applications of the nanostructure in the nonlinear optics and optoelectronic devices.

2. Materials Characterizations

We have prepared the sample by spin coating the triangular gold nanoplates (Nanjing JCNO Tech Co. Ltd) on the ITO glass. The gold nanoparticles were dispersed in an aqueous solution with optical density (OD) equal to 1, and the single piece of gold triangular is an equilateral triangular with side length (L) is 140 $\pm$ 25 nm, and the thickness is 8 $\pm$ 2 nm. Fig. 1(a) shows the measured absorption spectrum of the gold nanoplates by a UV-VIS-NIR spectrophotometer

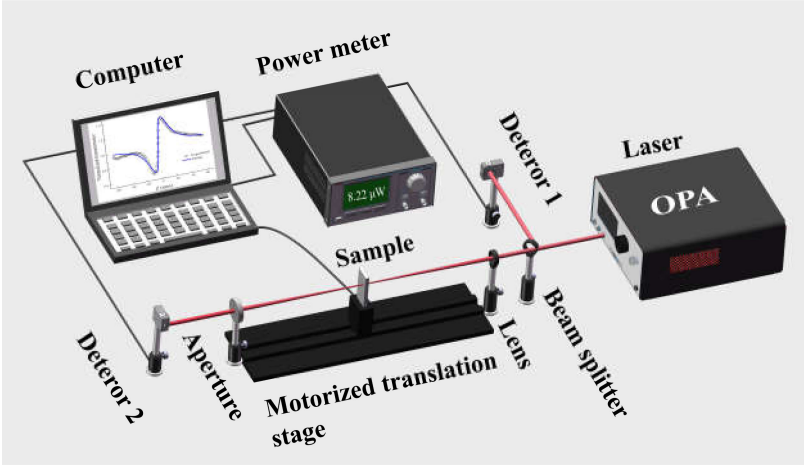

Fig. 2. The schematic diagram of the Z-scan system used for nonlinear optical measurement.

(UV-3600PLUS220/230VC, SHIMADZU), from which one can find that it has a relatively strong absorption near 780 nm wavelength, which corresponds to the quadrupole plasmon modes of gold triangular nanoparticle [42], [43]. We have calculated the extinction spectrum of a single gold triangular nanoparticle, as shown in the inset of Fig. 1(a). The extinction section is equal to the absorption section plus scatter section, and an extinction peak can be observed near 780 nm, indicating the resonance energy of the plasmon [44].

The ITO glass with excellent optical and electrical performance and 350 $\pm$ 30 nm thickness has been chosen as the substrate [45]. We dripped the gold solution onto the ITO glass, and used the spin coater to prepare a uniform structure, and finally left the sample in a dry environment for 24 hours until the aqueous solution evaporated. Fig. 1(b) show the SEM image of gold triangular nanoplates on ITO glass substrate, and we can find the dimer or trimer structure of the gold triangular nanoplates, as shown in the inset, where the local electric field enhancement effect of the trimer structure is usually much larger than the dimer and individual particles [47]. The distribution of the gold triangular nanoplates on ITO glass is mainly attributed to the concentration of Au dispersion solution, the rotation speed and time of the spin coater, etc. During the measurements, the Bruker D8 ADVANCE (Cu Kα) was used to obtain the XRD pattern of ITO glass and gold nanoplates/ITO hybrid structures, as shown in Fig. 1(c), which shows that the structure can preserve the nature of gold nanoplates and ITO glass. The temporal dynamics of the nonlinear response of the triangular gold has also been characterized by pump-probe method using 800 nm ultrafast pump light with power of 30 mW and 725 nm weak probe light, as depicted in Fig. 1(d). By fitting the experimental results [47], we obtained the lifetime constants with an initial fast relaxation time 5.4 ps and a slow relaxation time 130 ps, respectively.

3. Experimental Results and Discussions

The single beam Z-scan technique was employed to investigate the wavelength-dependent nonlinear optical response of the triangular gold nanostructure. The schematic diagram of the Z-scan system in the experiment is shown in Fig. 2. The laser source was an optical parametric amplifier pumped by a 800 nm Ti:sapphire amplifier system (Legend Elite, Coherent, USA) operating at a 1 kHz repetition rate and 35 fs pulse duration. By translating the sample along the optical axis of the focused laser beam, the sample will be exposed to different light intensities, and then we measured the transmittance of the sample under different light to study its nonlinear optical response.

We performed the open-aperture (OA) and closed-aperture (CA) Z-scan measurement from 650 to 900 nm wavelength with the incident intensity $\sim$9.1 GW/cm^2. The measured OA and CA/OA

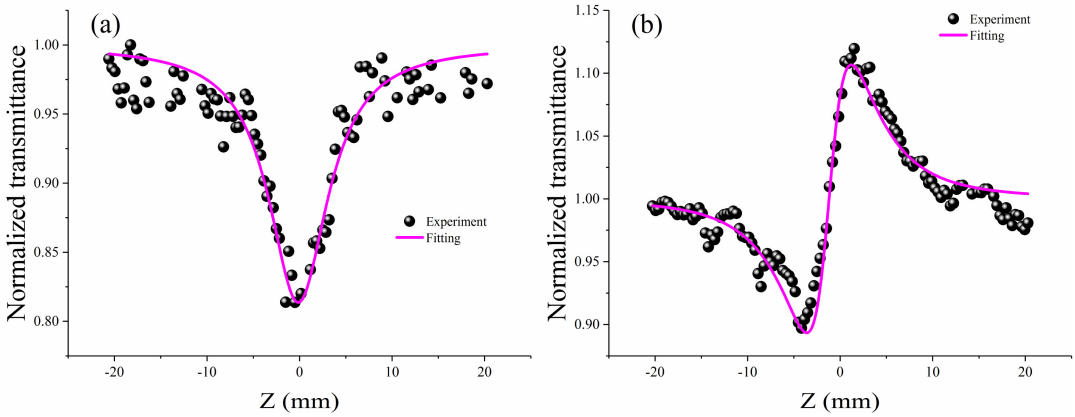

Fig. 3. The optical nonlinear response of the triangular gold on ITO glass. (a) The OA Z-scan results and (b) the CA/OA Z-scan results at 780 nm wavelength.

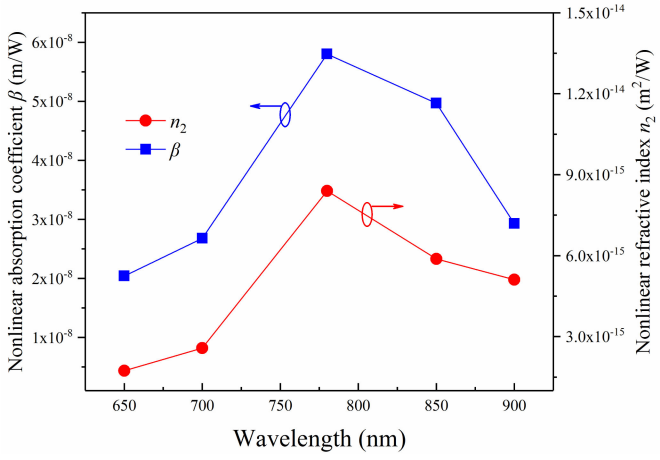

Fig. 4. The wavelength-dependent optical nonlinear response of the triangular gold on ITO glass.

results of the triangular gold on ITO glass are shown in Figs. 3(a) and 3(b), respectively. We used the following equations to fit the experimental data to obtain the nonlinear optical parameters [48]:

$$T_{open}(z) = 1 - \frac{q_0}{2\sqrt{2}(1 + z^2/z_0^2)} \tag{1}$$

$$T(x) = 1 + \frac{4x\Delta\Phi}{(1 + x^2)(9 + x^2)} \tag{2}$$

In Eq. (1), $q_0 = \beta I_0 L_{\text{eff}}$, where β is the nonlinear absorption coefficient, I_0 means the optical intensity at the focus, $L_{\text{eff}} = [1–e^{-\alpha L}]/\alpha$ is the sample's effective length, L is the sample length and α is the linear absorption coefficient [48]. In Eq. (2), T is the normalized transmittance, $x = z/z_0$ where $z_0 = \pi w_0{}^2/\lambda$ is the Rayleigh range and $\Delta\Phi = kn_2 I_0 L_{\text{eff}}$ means the focal nonlinear phase shift, $k = 2\pi/\lambda$ is the wavenumber [49]. By fitting the experimental data, we obtained the nonlinear refractive index n_2 is about 8.39 $\times$ 10^{-15} m^2/W, and the nonlinear absorption coefficient β is about 5.81 $\times$ 10^{-8} m/W at 780 nm excitation wavelength, indicting the reverse saturation absorption and self-focusing characteristics. We plotted the wavelength-dependent nonlinear optical response in Fig. 4, from which we observe that both the nonlinear refractive index and nonlinear absorption can be enhanced near 780 nm. Compared with the experimental results of triangular gold on ITO glass

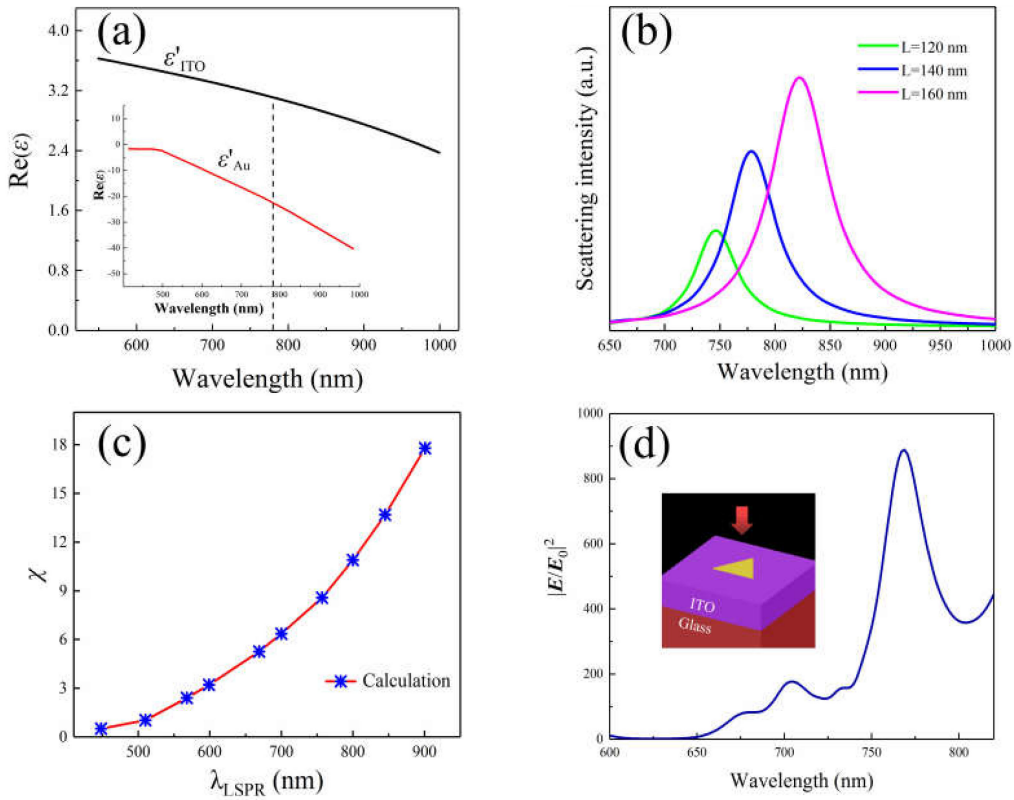

Fig. 5. (a) The wavelength-dependent real part of permittivity of ITO and Au, respectively. (b) The simulated size-dependent scattering spectra of the gold nanoparticle. (c) The relationship between the plasmon resonance wavelength and χ. (d) The wavelength-dependent electric field enhancement $|\boldsymbol{E}/\boldsymbol{E}_0|^2$ of a single Au nanoparticle between gold triangular and substrate interface, and the inset shows the simulation model.

at 650 nm, the maximum enhancement of nonlinear refractive index is 4.8 times and nonlinear absorption coefficient is 2.9 times, respectively. In addition, the measured maximum nonlinear refractive index n_2 is ~3 times larger than that reported by Rout et al. in gold nanoparticles thin film at 400 nm ($\lambda_{\mathrm{SPR}} = 520$ nm) [50] and two orders of magnitude larger than that by Wang et al. measured in a triangular-shaped gold nanoparticles array at 800 nm ($\lambda_{\mathrm{SPR}} = 566$ nm) [51].

To further investigate the nonlinear enhancement mechanism, we performed the numerical simulations with the dielectric constant of the gold triangular from [Ref. 52]. In addition, we used Drude model to describe ITO, $\varepsilon(\omega) = \varepsilon_\infty - \omega_{\mathrm{p}}{}^2/(\omega^2 + \mathrm{i}\gamma\omega)$, where a high-frequency permittivity of $\varepsilon_\infty = 3.8055$, a damping rate of $\gamma = 0.0468\omega_{\mathrm{p}}$, and a free-electron plasma frequency of $\omega_{\mathrm{p}}/2\pi = 473$ THz [6]. With the above considerations, we can obtain the permittivity of ITO and Au in Fig. 5(a). A conventional method to determine the plasmon resonance wavelength is to use the position of the scattering peaks of individual plasmonic nanostructures [53]–[55]. As depicted in Fig. 5(b), the position of scattering peaks of the triangular gold locates near 780 nm when the side length (L) equal to 140 nm, revealing that the plasmon resonance wavelength is near 780 nm. It can also be found that the plasmon resonance wavelength red-shifts when the side length increases, and the scattering intensity increases simultaneously. Another method can also be applied to analyze the LSPR [56] from the aspects of the extinction cross section $\boldsymbol{E}(\lambda) \propto \varepsilon_2(\lambda)/[(\varepsilon_1(\lambda) + \chi\varepsilon_{\mathrm{m}}(\lambda))^2 + \varepsilon_2(\lambda)^2]$, where $\varepsilon_1(\lambda)$ and $\varepsilon_2(\lambda)$ represent the real and the imaginary part of the permittivity of the metal, $\varepsilon_{\mathrm{m}}(\lambda)$ is the dielectric constant of the surrounding medium, and the factor of χ accounts for the nanoparticle shape [57]. When $\varepsilon_1(\lambda) + \chi\varepsilon_{\mathrm{m}}(\lambda) \approx 0$, the metal nanoparticles and incident light form the local surface electric field enhancement. We have calculated the relationship

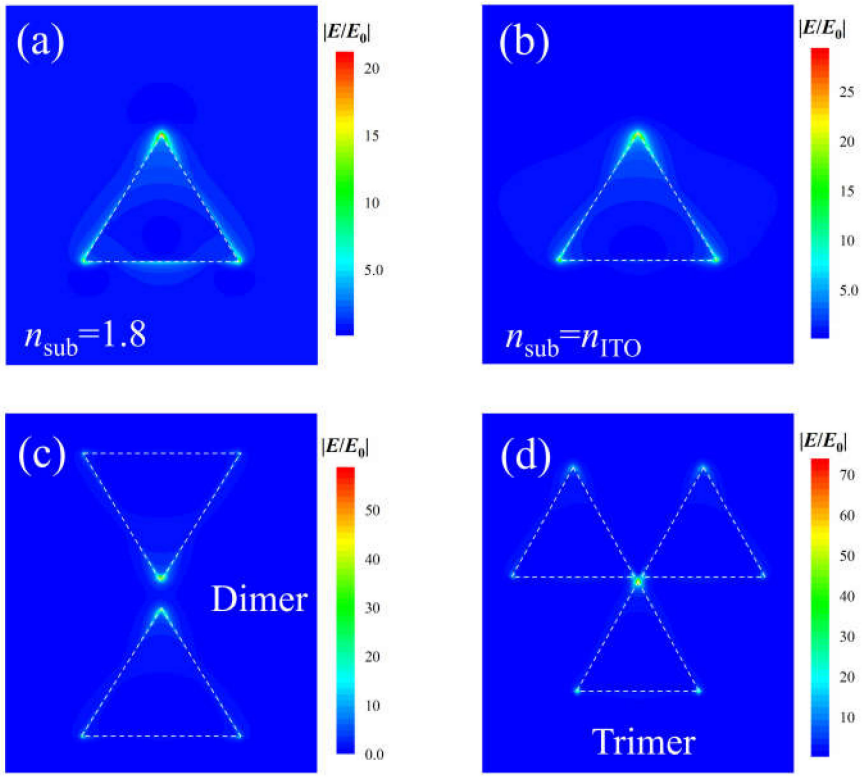

Fig. 6. The electric field distributions between (a) gold triangular and substrate interface, where the refractive index of substrate equal 1.8; (b) gold triangular and ITO glass interface; (c) gold triangular dimer and (d) trimer on ITO glass interface, $\lambda = 780$ nm.

between the plasmon resonance wavelength and χ of the structure, as shown in Fig. 5(c). The wavelength-dependent electric field enhancement $|\boldsymbol{E}/\boldsymbol{E}_0|^2$ for a single gold triangular nanoparticle between gold triangular and the substrate interface in Fig. 5(d) shows a resonance peak near 780 nm, where $|\boldsymbol{E}_0|$ is the amplitude of the incident light field.

The electric field $|\boldsymbol{E}/\boldsymbol{E}_0|$ distributions between gold triangular and the substrate interface at the 780 nm wavelength are shown in Fig. 6. Fig. 6(a) depicted the gold triangular nanoplates on the dielectric substrate, where its refractive index is equal to 1.8, larger than ITO glass, and the maximum electric field enhancement is about 21 times. While we replace the dielectric material for ITO, the maximum electric field enhancement can reach up to 30 times, as shown in Fig. 6(b). The interfaces show well-defined LSPR signals with high sensitivity to the dielectric constant of the surrounding medium [58]–[60]. In Figs. 6(c) and 6(d), the maximum electric field enhancement of the gold triangular dimer and trimer structure is up to 59 and 74 times, respectively. When the incident light field interacts with the medium, the variation in nonlinear refractive index of medium can be expressed as $\Delta n \propto \chi^{(3)'}|\boldsymbol{E}|^2$ and the nonlinear absorption as $\Delta\alpha \propto \chi^{(3)''}|\boldsymbol{E}|^2$, which are proportional to $|\boldsymbol{E}|^2$, where $\chi^{(3)'}$ and $\chi^{(3)''}$ are real part and imaginary part of the third order nonlinear polarizability, respectively. With the resonant field enhancement at LSPR region, the interaction of incident light with medium can be enhanced dramatically.

4. Conclusion

We have experimentally measured the broadband nonlinear optical response of the triangular gold nanoplates on ITO coated glass, and the measured nonlinear refractive index and nonlinear absorption coefficient can reach up to 8.39×10^{-15} m^2/W and 5.81×10^{-8} m/W, respectively. The

operating principle of the enhancement has been analyzed via numerical simulations, which can result from the plasmon resonance between the triangular gold nanoplates and the ITO substrate. The experimental results highlight the possibility to enhance the optical nonlinearity of the nanostructure, and may make inroads for the noble metals' potential applications in nonlinear optics and nanophotonics.

References

[1] Y. R. Shen, *The Principles of Nonlinear Optics.* New York, NY, USA: Wiley, 1984.
[2] R. W. Boyd, *Nonlinear Optics.* New York, NY, USA: Academic, 2003.
[3] G. P. Agrawal, *Applications of Nonlinear Fiber Optics.* London, U.K: Academic, 2001.
[4] B. E. A. Saleh and M. C. Teich, *Fundamentals of Photonics.* Hoboken NJ, USA: Wiley, 2007.
[5] E. Garmire, "Nonlinear optics in daily life," *Opt. Exp.*, vol. 21, no. 25, pp. 30532–30544, 2013.
[6] M. Z. Alam, I. De Leon, and R. W. Boyd, "Large optical nonlinearity of indium tin oxide in its epsilon-near-zero region," *Science*, vol. 352, no. 6287, pp. 795–797, 2016.
[7] J. Lee *et al.*, "Giant nonlinear response from plasmonic metasurfaces coupled to intersubband transitions," *Nature*, vol. 511, no. 7507, pp. 65–69, 2014.
[8] Y. M. Yang *et al.*, "Nonlinear Fano-resonant dielectric metasurfaces," *Nano Lett.*, vol. 15, no. 11, pp. 7388–7393, 2015.
[9] A. E. Minovich, A. E. Miroshnichenko, A. Y. Bykov, T. V. Murzina, D. N. Neshev, and Y. S. Kivshar, "Functional and nonlinear optical metasurfaces," *Laser. Photon. Res.*, vol. 9, no. 2, pp. 195–213, 2015.
[10] M. X. Ren *et al.*, "Nanostructured plasmonic medium for terahertz bandwidth all-optical switching," *Adv. Mater.*, vol. 23, no. 46, pp. 5540–5544, 2011.
[11] R. W. Boyd, R. J. Gehr, G. L. Fischer, and J. Sipe, "Nonlinear optical properties of nanocomposite materials," *J. Eur. Opt. Soc. A*, vol. 5, no. 5, pp. 505–512, 1996.
[12] R. W. Boyd and J. E. Sipe, "Nonlinear optical susceptibilities of layered composite materials," *J. Opt. Soc. Amer. B*, vol. 11, no. 2, pp. 297–303, 1994.
[13] A. K. Sarychev and V. M. Shalaev, "Electromagnetic field fluctuations and optical nonlinearities in metal-dielectric composites," *Phys. Rep.*, vol. 335, no. 6, pp. 275–371, 2000.
[14] M. Abb, P. Albella, J. Aizpurua, and O. L. Muskens, "All-optical control of a single plasmonic nanoantenna–ITO hybrid," *Nano Lett.*, vol. 11, no. 6, pp. 2457–2463, 2011.
[15] M. Abb, Y. D. Wang, C. De Groot, and O. L. Muskens, "Hotspot-mediated ultrafast nonlinear control of multifrequency plasmonic nanoantennas," *Nat. Commun.*, vol. 5, 2014, Art. no. 4869.
[16] N. M. Litchinitser and J. B. Sun, "Optical meta-atoms: Going nonlinear," *Science*, vol. 350, no. 6264, pp. 1033–1034, 2015.
[17] A. Rose, S. Larouche, E. Poutrina, and D. R. Smith, "Nonlinear magnetoelectric met amaterials: Analysis and homogenization via a microscopic coupled-mode theory," *Phys. Rev. A*, vol. 86, no. 3, 2012, Art. no. 033816.
[18] A. Rose, D. Huang, and D. R. Smith, "Nonlinear interference and unidirectional wave mixing in metamaterials," *Phys. Rev. Lett.*, vol. 110, no. 6, 2013, Art. no. 063901.
[19] J. Obermeier, T. Schumacher, and M. Lippitz, "Nonlinear spectroscopy of plasmonic nanoparticles," *Adv. Phys. X*, vol. 3, no. 1, 2018, Art. no. 1454341.
[20] H. Aouani, M. Rahmani, M. Navarro-Cía, and S. A. Maier, "Third-harmonic-upconversion enhancement from a single semiconductor nanoparticle coupled to a plasmonic antenna," *Nature Nanotech.*, vol. 9, no. 4, pp. 290–294, 2014.
[21] M. Celebrano *et al.*, "Mode matching in multiresonant plasmonic nanoantennas for enhanced second harmonic generation," *Nature Nanotech.*, vol. 10, no. 5, pp. 412–417, 2015.
[22] B. Metzger, L. Gui, J. Fuchs, D. Floess, M. Hentschel, and H. Giessen, "Strong enhancement of second harmonic emission by plasmonic resonances at the second harmonic wavelength," *Nano Lett.*, vol. 15, no. 6, pp. 3917–3922, 2015.
[23] B. Metzger, L. Gui, and H. Giessen, "Ultrabroadband chirped pulse second-harmonic spectroscopy: Measuring the frequency-dependent second-order response of different metal films," *Opt. Lett.*, vol. 39, no. 18, pp. 5293–5296, 2014.
[24] I. Tanahashi, Y. Manabe, T. Tohda, S. Sasaki, and A. Nakamura, "Optical nonlinearities of Au/SiO_2 composite thin films prepared by a sputtering method," *J. Appl. Phys.*, vol. 79, no. 3, pp. 1244–1249, 1996.
[25] V. I. Savinkov, G. Y. Shakhgil'dyan, A. Paleari, and V. N. Sigaev, "Synthesis of optically uniform glasses containing gold nanoparticles: Spectral and nonlinear optical properties," *Glass Ceram.*, vol. 70, no. 3, pp. 143–148, 2013.
[26] E. Hutter and J. H. Fendler, "Exploitation of localized surface plasmon resonance," *Adv. Mater.*, vol. 16, no. 19, pp. 1685–1706, 2004.
[27] R. C. Jin, Y. W. Cao, C. A. Mirkin, K. Kelly, G. C. Schatz, and J. Zheng, "Photoinduced conversion of silver nanospheres to nanoprisms," *Science*, vol. 294, no. 5548, pp. 1901–1903, 2001.
[28] A. J. Haes, S. L. Zou, G. C. Schatz, and R. P. Van Duyne, "Nanoscale optical biosensor: Short range distance dependence of the localized surface plasmon resonance of noble metal nanoparticles," *J. Phys. Chem. B*, vol. 108, no. 22, pp. 6961–6968, 2004.
[29] T. R. Jensen, M. D. Malinsky, C. L. Haynes, and R. P. Van Duyne, "Nanosphere lithography: Tunable localized surface plasmon resonance spectra of silver nanoparticles," *J. Phys. Chem. B*, vol. 104, no. 45, pp. 10549–10556, 2000.
[30] N. L. Rosi and C. A. Mirkin, "Nanostructures in biodiagnostics," *Chem. Rev.*, vol. 105, no. 4, pp. 1547–1562, 2005.
[31] N. Ahmadi, R. Poursalehi, A. Kirilyuk, and M. K. Moravvej-Farshi, "Effect of gold plasmonic shell on nonlinear optical characteristics and structure of iron based nanoparticles," *Appl. Surf. Sci.*, vol. 479, pp. 114–118, 2019.

[32] Y. Fu, R. A. Ganeev, P. Krishnendu, C. Y. Zhou, K. S. Rao, and C. L. Guo, "Size-dependent off-resonant nonlinear optical properties of gold nanoparticles and demonstration of efficient optical limiting," *Opt. Mater. Exp.*, vol. 9, no. 3, pp. 976–991, 2019.
[33] A. Rout *et al.*, "Nonlinear optical studies of gold nanoparticle films," *Nanomaterials*, vol. 9, no. 2, 2019, Art. no. 291.
[34] K. D. Ko *et al.*, "Nonlinear optical response from arrays of au bowtie nanoantennas," *Nano Lett.*, vol. 11, no. 1, pp. 61–65, 2011.
[35] B. Metzger *et al.*, "Doubling the efficiency of third harmonic generation by positioning ITO nanocrystals into the hot-spot of plasmonic gap-antennas," *Nano Lett.*, vol. 14, no. 5, pp. 2867–2872, 2014.
[36] M. Z. Alam, S. A. Schulz, J. Upham, I. De Leon, and R. W. Boyd, "Large optical nonlinearity of nanoantennas coupled to an epsilon-near-zero material," *Nat. Photon.*, vol. 12, no. 2, 2018, Art. no. 79.
[37] G. F. Ferbonink, E. R. Spada, D. P. D. Santos, M. L. Sartorelli, and R. A. Nome, "Ultrafast dynamics of au nanopyramid interfaces prepared by nanosphere lithography: Effect of substrate chemical composition," *J. Braz. Chem. Soc.*, vol. 27, no. 2, pp. 423–433, 2016.
[38] J. Stotter, Y. Show, S. H. Wang, and G. Swain, "Comparison of the electrical, optical, and electrochemical properties of diamond and indium tin oxide thin-film electrodes," *Chem. Mater.*, vol. 17, no. 19, pp. 4880–4888, 2005.
[39] H. Hillebrandt and M. Tanaka, "Electrochemical characterization of self-assembled alkylsiloxane monolayers on indium-tin oxide (ITO) semiconductor electrodes," *J. Phys. Chem. B*, vol. 105, no. 19, pp. 4270–4276, 2001.
[40] J. Davenas, S. Besbes, and H. B. Ouada, "NIR spectrophotometry characterization of ITO electronic property changes at the interface with a PPV derivative," *Synth. Met.*, vol. 138, no. 1-2, pp. 295–298, 2003.
[41] M. T. Bhatti, A. M. Rana, and A. F. Khan, "Characterization of rf-sputtered indium tin oxide thin films," *Mater. Chem. Phys.*, vol. 84, no. 1, pp. 126–130, 2004.
[42] J. Zhu, H. Liu, and L. Q. Huang, "Wall thickness dependent double optical bistability in gold nanotube: A physical mechanism based on local field enhancement," *J. Appl. Phys.*, vol. 105, no. 11, 2009, Art. no. 114319.
[43] Z. Li *et al.*, "Ultrafast third-order optical nonlinearity in au triangular nanoprism with strong dipole and quadrupole plasmon resonance," *J. Phys. Chem. C*, vol. 117, no. 39, pp. 20127–20132, 2013.
[44] P. Jiang, C. Li, Y. Y. Chen, G. Song, Y. L. Wang, and L. Yu, "Strong exciton-plasmon coupling and hybridization of organic-inorganic exciton-polaritons in plasmonic nanocavity," *Chin. Phys. Lett.*, vol. 36, no. 10, 2019, Art. no. 107301.
[45] Z. Ma, Z. Li, K. Liu, C. Ye, and V. J. Sorger, "Indium-tin oxide for high-performance electro-optic modulation," *Nanophotonics*, vol. 4, pp. 198–213, 2015.
[46] A. L. Koh, A. I. Fernández-Domínguez, D. W. McComb, S. A. Maier, and J. K. W. Yang, "High-resolution mapping of electron-beam-excited plasmon modes in lithographically defined gold nanostructures," *Nano Lett.*, vol. 11, no. 3, pp. 1323–1330, 2011.
[47] J. Li *et al.*, "Nonlinear optical response in natural van der waals heterostructures," *Adv. Opt. Mater.*, vol. 8, no.no. 15, 2020, Art. no. 2000382.
[48] M. Sheik-Bahae, A. A. Said, and E. W. Van Stryland, "High-sensitivity, single-beam n_2 measurements," *Opt. Lett.*, vol.vol. 14, no. 17, pp. 955–957, 1989.
[49] J. Yi, L. L. Miao, J. Li, W. Hu, C. J. Zhao, and S. C. Wen, "Third-order nonlinear optical response of $CH_3NH_3PbI_3$ perovskite in the mid-infrared regime," *Opt. Mater. Exp.*, vol. 7, no. 11, pp. 3894–3901, 2017.
[50] A. Rout *et al.*, "Nonlinear optical studies of gold nanoparticle films," *Nanomaterials*, vol. 9, no. 2, 2019, Art. no. 291.
[51] K. Wang, H. Long, M. Fu, G. Yang, and P. Lu, "Intensity-dependent reversal of nonlinearity sign in a gold nanoparticle array," *Opt. Lett.*, vol. 35, no. 10, pp. 1560–1562, 2010.
[52] P. B. Johnson and R. W. Christy, "Optical constants of the noble metals," *Phys. Rev. B*, vol. 6, no. 12, 1972, Art. no. 4370.
[53] K. H. Su, Q. H. Wei, and X. Zhang, "Tunable and augmented plasmon resonances of Au/Sio_2/Au nanodisks," *Appl. Phys. Lett.*, vol. 88, no. 6, 2006, Art. no. 063118.
[54] W. Chen, H. T. Hu, W. Jiang, Y. H. Xu, S. P. Zhang, and H. X. Xu, "Ultrasensitive nanosensors based on localized surface plasmon resonances: From theory to applications," *Chin. Phys. B.*, vol. 27, no. 10, 2018, Art. no. 107403.
[55] H. Feng *et al.*, "Ultra-large local field enhancement effect of isolated thick triangular silver nanoplates on a silicon substrate in the green waveband," *Opt. Lett.*, vol. 45, no. 7, pp. 2099–2102, 2020.
[56] K. A. Willets and R. P. Van Duyne, "Localized surface plasmon resonance spectroscopy and sensing," *Annu. Rev. Phys. Chem.*, vol. 58, no. 1, pp. 267–297, 2007.
[57] K. L. Kelly, E. Coronado, L. L. Zhao, and G. C. Schatz, "The optical properties of metal nanoparticles: the influence of size, shape, and dielectric environment," *J. Phys. Chem. B*, vol. 107, no. 3, pp. 668–677, 2003.
[58] C. Z. Fang, Y. Liu, G. Q. Han, Y. Shao, J. C. Zhang, and Y. Hao, "Localized plasmon resonances for black phosphorus bowtie nanoantennas at terahertz frequencies," *Opt. Exp.*, vol. 26, no. 21, pp. 27683–27693, 2018.
[59] T. R. Jensen, G. C. Schatz, and R. P. Van Duyne, "Nanosphere lithography: Surface plasmon resonance spectrum of a periodic array of silver nanoparticles by ultraviolet-visible extinction spectroscopy and electrodynamic modeling," *J. Phys. Chem. B*, vol. 103, no. 13, pp. 2394–2401, 1999.
[60] J. J. Mock, D. R. Smith, and S. Schultz, "Local refractive index dependence of plasmon resonance spectra from individual nanoparticles," *Nano Lett.*, vol, vol. 3, no. 4, pp. 485–491, 2003.